

ansa-Bis(fluorenyl)neodymium Catalysts for Cyclocopolymerization of Ethylene with Butadiene

Julien Thuilliez,[†] Louis Ricard,[‡] François Nief,[‡] Fernande Boisson,[§] and Christophe Boisson^{*,*†}

Université de Lyon, Univ. Lyon 1, CPE Lyon, CNRS UMR 5265 Laboratoire de Chimie Catalyse Polymères et Procédés (C2P2), LCPP team-Bat 308F, 43 Bd du 11 novembre 1918, F-69616 Villeurbanne, France, Service de RMN du Réseau des Polyméristes Lyonnais CNRS UMR5223-Echangeur de Solaize, Chemin du canal 69360 Solaize, France, and Laboratoire Hétéroéléments et Coordination CNRS UMR 7653-DCPH, Ecole Polytechnique, 91128 Palaiseau, France

Received February 19, 2009; Revised Manuscript Received April 1, 2009

ABSTRACT: Metallocene borohydride complexes $\{(\text{Me}_2\text{Si}(\text{C}_{13}\text{H}_8)_2)\text{Nd}(\mu\text{-BH}_4)[(\mu\text{-BH}_4)\text{Li}(\text{THF})]_2\}$ (**1**) and $(\text{Me}_2\text{Si}(2,7\text{-}t\text{Bu}_2\text{C}_{13}\text{H}_6)_2)\text{Nd}(\text{BH}_4)(\mu\text{-BH}_4)\text{Li}(\text{ether})_3$ (**2**) were prepared by reaction of the dilithium salts of silylene-bridged bis(fluorenyl) ligands with the borohydride precursor $\text{Nd}(\text{BH}_4)_3(\text{THF})_3$. The solid state structures of dimeric **1** and monomeric **2** ate complexes were established by X-ray diffraction studies. We showed that these complexes used in combination with $(n\text{Bu})(n\text{Oct})\text{Mg}$ are highly efficient for cyclocopolymerization of ethylene with butadiene leading to a new class of elastomers. Catalyst **1**/ $(n\text{Bu})(n\text{Oct})\text{Mg}$ provided elastomers with a polyethylene skeleton incorporating unsaturated groups (trans double bond and pendant vinyl units) and 1,2-cyclohexane rings. These rings are formed via an intramolecular cyclization which occurs with a high *trans* selectivity. The investigation of catalyst **2**/ $(n\text{Bu})(n\text{Oct})\text{Mg}$ has revealed that the tertio-butyl substitution in positions 2 and 7 of fluorenyl ligands influenced the microstructure of copolymers since in addition to 1,2-cyclohexane rings, 1,4-cyclohexane rings were formed. This original microstructure was characterized using 2D NMR $^1\text{H}\text{-}^1\text{H}$ and $^1\text{H}\text{-}^{13}\text{C}$ with direct and long-range correlations. Mechanisms of stereoselective formation of *trans*-1,2-cyclohexane and *trans*-1,4-cyclohexane rings were fully investigated.

Introduction

The use of tailor-made single-site catalysts instead of traditional Phillips and Ziegler–Natta catalysts for olefin polymerization enabled both the development of new ranges of commodity polyolefins (polyethylenes, polypropylene) and also the preparation of new specialty polymers.¹ Concerning this latter topic, an appropriate strategy consists in incorporating chemical moieties with remarkable microstructure in the polyolefin backbone.

For example, the incorporation of cyclic units in polyolefin backbones greatly influences the physical properties of polyolefins leading to new materials with wide ranges of applications as shown by the industrial availability of cycloolefin copolymers (COC). Two main strategies have been adopted to prepare polymers bearing cyclic units. The first method consists to homo- and copolymerize cycloolefins using in particular metallocene catalysts² and the second one is based on the cyclopolymerization of nonconjugated dienes such as 1,4-pentadiene, 1,5-hexadiene, or 1,6-heptadiene.³ The cyclocopolymerization of ethylene with butadiene can also lead to ring formation. This reaction is more challenging as copolymerization of olefins and conjugated dienes is very difficult. In addition, since rings formation requires vinyl units, it is also necessary to be able to control the regioselectivity of the diene insertion (1,2 versus 1,4 insertion). However, when these requirements are fulfilled, copolymers obtained by cyclocopolymerization of olefins with butadiene are very attractive materials since they may possess in addition to rings, unsaturated groups in the polymer backbone. Applications in the field of vulcanizable rubber are then expected.

The cyclocopolymerization of ethylene with butadiene using group 4 metallocene have been investigated in detail recently.⁴ The formation of cyclopropane and cyclopentane rings via 1,2-butadiene units has been described. Nevertheless, no or few unsaturations (1,4-units) are obtained in the polymer backbone and the polymerization activity decreases by increasing the butadiene content in the polymerization medium. Interestingly, polyethylenes containing cyclopropane rings have been used to obtain cross-linked polyethylene.⁵ During the past decade, our group has developed efficient neodymium metallocene catalysts for the copolymerization of ethylene with butadiene.⁶ In most cases, butadiene units are mainly *trans*-1,4-inserted and statistical or alternating copolymers are obtained.⁷ In addition, new elastomers containing *trans*-1,4 units, 1,2-units and unprecedented *trans*-1,2-cyclohexane rings have been prepared.⁸ The fundamental difference of behavior between neodymium and group 4 metallocenes concerns the regioselectivity of butadiene insertion. In the case of group 4 metallocenes, butadiene is 1,2-inserted “as an α -olefin” and cyclopentane (or cyclopropane) rings are formed. Concerning neodymium catalysts the cyclization occurs after a classical 2,1-insertion of butadiene (via an η^3 -butenyl intermediate) leading to the formation of 1,2-cyclohexane rings.

We have called EBR (ethylene–butadiene rubber) the new elastomers incorporating cyclohexane rings.⁹ The potential of these new elastomers is important and in particular as new rubbers for the tire industry. In comparison with EPDM, an improved covulcanization with other rubber materials is expected since they possess unsaturated groups in the polymer backbone. In addition, these new elastomers are obtained with readily available monomers (only ethylene and butadiene) and further their preparation is thus of great importance. Recently, the use of borohydride precursors as an alternative to chloride neodymium derivatives for the polymerization of ethylene and conjugated dienes has been developed.¹⁰ It appears that the

* Corresponding author. E-mail: boisson@lcpp.cpe.fr.

[†] Université de Lyon.

[‡] Ecole Polytechnique.

[§] Service de RMN.

neodymium borohydride chemistry is very rich since it gives access to well-defined neodymocenes but also to original derivatives when chloride analogues cannot be obtained. The preparation of borohydride neodymocene complexes is thus of interest especially with the aim to fully investigate the unique mechanism of cyclocopolymerization of ethylene with butadiene observed using silylene bis(fluorenyl)neodymium catalysts but also to establish relationships between the ligand structures and the polymerization mechanism. In the present article, we report the synthesis and the characterization of complexes $\{(\text{Me}_2\text{Si}(\text{C}_{13}\text{H}_9)_2)\text{Nd}(\mu\text{-BH}_4)[(\mu\text{-BH}_4)\text{Li}(\text{THF})]_2\}$ (**1**) and $(\text{Me}_2\text{Si}(2,7\text{-}t\text{Bu}_2\text{C}_{13}\text{H}_6)_2)\text{Nd}(\text{BH}_4)(\mu\text{-BH}_4)\text{Li}(\text{ether})_3$ (**2**) and their successful use for cyclocopolymerization of ethylene with butadiene. In addition, we also report unprecedented polymer microstructures and investigate in detail the mechanisms of ring formation and the cyclization stereochemistry.

Experimental Section

Materials. All syntheses were performed under pure and dry argon, using the standard Schlenk techniques or a glovebox. Tetrahydrofuran and pentane were distilled over sodium/benzophenone prior to use. Toluene and *n*-heptane were dried on 3 Å molecular sieves. Deuterated solvents used for ^1H NMR analysis of air- and moisture-sensitive compounds were distilled over sodium.

Synthesis of $\text{Me}_2\text{Si}(\text{C}_{13}\text{H}_9)_2$. A 3.15 mL aliquot of Me_2SiCl_2 (26 mmol) was slowly added to a THF solution (250 mL) of $[\text{C}_{13}\text{H}_9]\text{Li}$ (8.95 g, 52 mmol) at -30°C . The temperature was raised to 20°C , and the solution was then stirred for 15 h. The solvent was evaporated to dryness and the residue was extracted with 50 mL of toluene. After evaporation of the solvent an orange powder was obtained. The product was then washed with cold heptane (3*25 mL). The solid was then heated at 85°C under vacuum in order to sublimate residual fluorene. The product was isolated as a white powder (8.19 g, 81%).

^1H NMR (22°C , benzene- d_6 , 300 MHz): δ -0.56 (s, 6H, Si- CH_3), 4.18 (s, 2H, Si- CH in C_{13}H_9), 7.15 (t, J 8 Hz, 4H, CH in C_{13}H_9), 7.27 (t, J 8 Hz, 4H, CH in C_{13}H_9), 7.38 (d, J 8 Hz, 4H, CH in C_{13}H_9), 7.80 (d, J 8 Hz, 4H, CH in C_{13}H_9).

Synthesis of $[\text{Me}_2\text{Si}(\text{C}_{13}\text{H}_9)_2]\text{Li}_2$. Butyllithium (1.6 M solution, 11.8 mL, 18.4 mmol) was added to a 100 mL toluene solution containing $\text{Me}_2\text{Si}(\text{C}_{13}\text{H}_9)_2$ (3.67 g, 9.4 mmol) at -30°C . The mixture was stirred for 15 h at ambient temperature then the temperature was raised to 80°C and the mixture was stirred for 3 h more. The temperature was decreased to ambient temperature, the solution was filtered and the solvent was evaporated. The product was washed with cold heptane (2×25 mL). $[\text{Me}_2\text{Si}(\text{C}_{13}\text{H}_9)_2]\text{Li}_2$ was isolated as a yellow powder (2.57 g, 68%).

^1H NMR (22°C , THF- d_8 , 300 MHz): δ 0.90 ppm (s, 6H, Si- CH_3), 6.54 ppm (t, J 8 Hz, 4H, CH in C_{13}H_9), 6.91 ppm (t, J 8 Hz, 4H, CH in C_{13}H_9), 7.91 (d, J 8 Hz, 4H, CH in C_{13}H_9), 7.98 (d, J 8 Hz, CH in C_{13}H_9).

^1H NMR (22°C , pyridine- d_5 , 300 MHz): δ 1.55 (s, 6H, Si- CH_3), 6.94 (m, 4H, CH in C_{13}H_8), 7.15 (m, 4H, CH in C_{13}H_8), 8.59 (d, J 8 Hz, 4H, CH in C_{13}H_8), 8.72 (d, J 8 Hz, 4H, CH in C_{13}H_8).

Synthesis of $\{(\text{Me}_2\text{Si}(\text{C}_{13}\text{H}_9)_2)\text{Nd}(\mu\text{-BH}_4)[(\mu\text{-BH}_4)\text{Li}(\text{THF})]_2\}$ (1**).** A diethyl ether solution (75 mL) containing $[\text{Me}_2\text{Si}(\text{C}_{13}\text{H}_9)_2]\text{Li}_2$ (0.515 g, 1.3 mmol) was added to a diethyl ether solution (75 mL) containing of $\text{Nd}(\text{BH}_4)_3(\text{THF})_3$ (0.521 g, 1.3 mmol). The mixture was stirred for 12 h at ambient temperature. The solution is filtrated and concentrated to a volume of 125 mL. Addition of 200 mL of pentane caused precipitation of red crystals of **1** (360 mg, 41%).

Anal. Calcd for $(\text{NdC}_{32}\text{H}_{38}\text{OSiB}_2\text{Li})_2$ (639.5) $_n$: C, 60.10; H, 5.99. Found: C, 59.86; H, 6.29.

^1H NMR (22°C , THF- d_8 , 300 MHz): δ -2.35 (br, $2 \times 4\text{H}$, CH in C_{13}H_8), 5.0 (br, 4H, CH in C_{13}H_8), 13.15 (br, 6H, Si- CH_3), 97.5 (vbr, 8H, $\text{Nd}(\text{BH}_4)_2$). Last CH resonance of fluorenyl ligands is overlapped with one signal of THF (3.6 ppm).

Synthesis of $[\text{Me}_2\text{Si}(2,7\text{-}t\text{Bu}_2\text{C}_{13}\text{H}_6)_2][\text{Li}(\text{THF})]_2$. Me_2SiCl_2 (6.4 mmol) was slowly added to a THF solution (150 mL) of $[2,7\text{-}$

$t\text{Bu}_2\text{C}_{13}\text{H}_7]\text{Li}$ (3.64 g, 12.8 mmol) at -50°C . The temperature was raised to 20°C and the solution was then stirred for 15 h. The solvent was evaporated to dryness and the residue was extracted with 50 mL of toluene. After evaporation of the solvent a beige solid was obtained. This product was dissolved in 50 mL of THF. The temperature was then decreased to 0°C and 8.0 mL of a solution of butyllithium (1.6 M solution, 12.8 mmol) was added. The mixture was stirred for 15 h at ambient temperature. The solvent was evaporated to dryness and the product was washed with cold heptane (2×25 mL). $[\text{Me}_2\text{Si}(2,7\text{-}t\text{Bu}_2\text{C}_{13}\text{H}_6)_2][\text{Li}(\text{THF})]_2$ was thus isolated (4.8 g, 97%).

^1H NMR (22°C , THF- d_8 , 300 MHz): δ 0.96 (s, 6H, Si- CH_3), 1.39 (s, 36H, $t\text{Bu}$); 1.78 and 3.62 (m, $2 \times 8\text{H}$, $2 \times \text{THF}$), 6.65 (d, $J = 8$ Hz, 4H, CH), 7.78 (d, $J = 8$ Hz, 4H, CH), 8.02 (s, 4H, CH).

Synthesis of $(\text{Me}_2\text{Si}(2,7\text{-}t\text{Bu}_2\text{C}_{13}\text{H}_6)_2)\text{Nd}(\text{BH}_4)(\mu\text{-BH}_4)\text{Li}(\text{ether})_3$ (2**).** A THF solution (75 mL) containing $[\text{Me}_2\text{Si}(2,7\text{-}t\text{Bu}_2\text{C}_{13}\text{H}_6)_2]\text{Li}_2(\text{THF})_2$ (6.4 mmol) was added to a THF solution (75 mL) containing of $\text{Nd}(\text{BH}_4)_3(\text{THF})_3$ (2.59 g, 6.4 mmol). The mixture was stirred for 15 h at ambient temperature. The solvent was evaporated to dryness, then 175 mL of diethyl ether were added. The solution was filtrated and concentrated to a volume of 75 mL. Addition of 75 mL of pentane caused precipitation of **2** (2.45 g, 38%).

^1H NMR (22°C , THF- d_8 , 300 MHz): δ -3.34 (br, 36H, $t\text{Bu}$), -2.02 (br, 4H, CH in C_{13}H_6), -0.74 (br, 4H, CH in C_{13}H_6), 12.89 (br, 6H, Si- CH_3)—a very broad signal was detected around 90 ppm.

Polymerization Procedure. Polymerizations were performed in a 250 mL glass reactor equipped with a stainless steel blade stirrer and an external water jacket for temperature control. The alkylating agent and the neodymium precursor were introduced in a flask containing 200 mL of toluene. The mixture was stirred for 10 min, and finally transferred in the reactor under a stream of argon. The argon was then pumped out before introducing the monomer(s) (ethylene, butadiene or ethylene-butadiene gaseous mixture). Temperature and pressure were then progressively increased up to 80°C and 4 bar respectively, and kept constant. At the end of polymerization, the mixture was quenched with 1 mL of methanol. The polymer was then precipitated out with methanol, washed, and dried under vacuum.

Polymerization at higher monomer concentrations (runs 5 and 6) were performed in a 1 L stainless steel reactor, equipped with a stainless steel blade stirrer and an external water jacket for temperature control. The desired amount of butadiene was dissolved in 400 mL of cold toluene. A toluene solution (200 mL) of the alkylating agent and the neodymium complex was prepared at room temperature. The two aforementioned solutions were transferred successively into the reactor. The reactor was charged with ethylene and heated up to 80°C . The polymerization is then performed without monomer addition. The polymer was precipitated in methanol, washed, and dried under vacuum.

Characterizations. Elemental analyses were obtained with a Fisons EA 1108 CHON apparatus at the Service d'Analyses de l'Université de Dijon.

NMR spectra of metallic complexes were obtained with a Bruker AC 300 spectrometer. Microstructures of polymers were determined by NMR using a Bruker DRX 400 spectrometer operating at 400 MHz for ^1H and 100.6 MHz for ^{13}C . 1D ^1H and ^{13}C spectra were obtained with a 5 mm QNP probe at 353 K. A 2:1 volume mixture of tetrachloroethylene and perdeuterobenzene was used as solvent. 2D NMR spectra were recorded at 333K with a broadband probe with field gradients in the z -axis. gs-COSY sequence was used for ^1H - ^1H correlations, and gs-HMQC and gs-HMBC sequences were used for ^1H - ^{13}C correlations.

Gel permeation chromatography data were obtained in THF solutions using a Waters apparatus including a Waters 515 HPLC pump, a series of columns (1 precolumn PL Gel $5\ \mu\text{m}$; 2 columns PL Gel $5\ \mu\text{m}$ Mixte C and 1 column PL Gel $5\ \mu\text{m}$ -500 Å), and a Waters 410 refractometer detector. Column temperature and flow

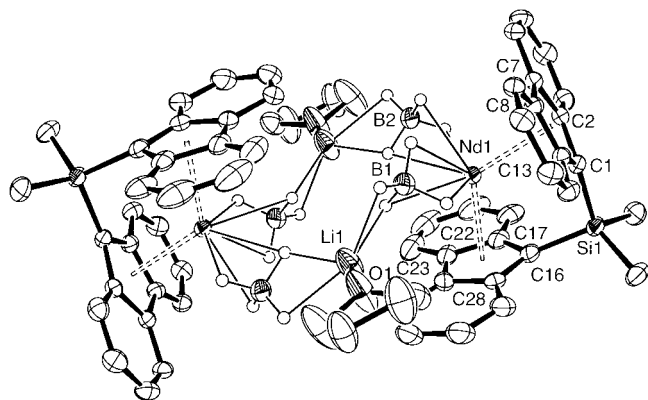


Figure 1. ORTEP plot of **1** (ellipsoids scaled at 50%). The hydrogen atoms (except on the borohydrides) have been omitted for clarity. Selected distances (Å) and angles (deg): Nd(1)–C(1) = 2.671(2); Nd(1)–C(16) = 2.686(2); Nd(1)–C(2) = 2.726(2); Nd(1)–C(28) = 2.748(2); Nd(1)–C(13) = 2.801(2); Nd(1)–C(17) = 2.812(2); Nd(1)–C(7) = 2.882(2); Nd(1)–C(23) = 2.905(2); Nd(1)–C(8) = 2.928(2); Nd(1)–C(22) = 2.939(2); Si(1)–C(16) = 1.866(3); Si(1)–C(1) = 1.866(2); Nd(1)–B(2) = 2.664(3); Nd(1)–B(1) = 2.664(3); B(2)–Nd(1)–B(1) = 94.6(1); C(16)–Si(1)–C(1) = 100.9(1).

rate were respectively 45 °C and 1 mL/mn. The system was calibrated using polystyrene standards.

Differential scanning calorimetry measurements were performed on a Setaram DSC 131 apparatus. Samples were heated from –120 to +150 °C at 10 °C min⁻¹. Two successive heating and cooling of the samples were performed (10 °C min⁻¹). We have considered data obtained during the second run.

RX structures were recorded with an Enraf Nonius KappaCCD diffractometer at 150 K, using Mo K α radiation ($\lambda = 0.71069$ Å).

Results and Discussion

Synthesis and Characterization of Borohydride Catalyst Precursors. The compound Nd(BH₄)₃(THF)₃ (**3**) is known to be an excellent precursor in view of the preparation of organometallic borohydride complexes of neodymium.¹¹ The synthesis of such complexes proceeds via a salt metathesis reaction between an alkali metal salt and the borohydride complex **3** in THF or Et₂O. Using this strategy, complex **1** and **2** were obtained from the reaction of respectively [Me₂Si(C₁₃H₈)₂]₂Li₂ and [Me₂Si(2,7-*t*BuC₁₃H₆)₂][Li(THF)]₂ with **3**.

Suitable crystals of **1** for X-ray diffraction analysis were grown from a solution of THF/pentane. An ORTEP plot is presented in Figure 1.

This figure reveals the dimeric and centrosymmetric nature of the anionic ate-complex **1**: Only one THF molecule is bonded to the lithium atom and its coordination sphere is completed with two bidentate borohydrides. One can also note a short distance between lithium and one carbon belonging to the 6-membered ring on the fluorenyl ligand [Li(1)–C(25)#2 = 2.633(7) Å]. As for the neodymium atom, it is sandwiched between the two fluorenyl moieties of the bridging ligand and bonded with two bridging borohydrides in the usual tridentate way.

The Nd–C(fluorenyl) distances span widely from 2.67 to 2.94 Å, the shortest bonds being between Nd and the carbon atoms C(1) and C(16) directly bonded to the bridge. According to the most recent estimates,¹² the value of the mean Nd–C bond length, defined as the sum of the Nd and C covalent radii, is 2.74(8) Å. Using this criterion, all Nd–C(5-membered ring) distances in **1** fall within the range of a bond (with the usual margin of 3 times the esd value) and therefore the *ansa*-bis(fluorenyl) ligand is best described as bis- $[\eta^7]$ bonded to Nd. Interestingly, coordination mode of fluorenyl ligands has been discussed by Carpentier *et al.* in a review dealing with groups 2 and 3 metal complexes incorporating fluorenyl ligands.¹³

There are a number of related rare earth complexes with silicon-bridged mixed Cp-fluorenyl ligands such as Flu–SiMe₂–Cp (L¹) and (Flu–SiMe₂–C₅Me₄) (L²) that have been structurally characterized: (L¹)DyN(SiMe₃)₂, (L¹)DyCH(SiMe₃)₂,¹⁴ (L¹)Y(allyl)(THF),¹⁵ and (L²)YN(SiMe₃)₂,¹⁶ and also neodymium complexes with carbon-bridged mixed Cp-fluorenyl ligands like Flu–CMe₂–Cp (L³) and (Flu–CMe₂–C₅H₃*t*Bu) (L⁴): (L²)Nd(allyl)(THF) and (L³)Nd(allyl)(THF).¹⁵ All these complexes display the same bonding pattern of the metal to the fluorenyl ring carbon atoms as in **1**: the shortest distance is with the carbon closest to the bridge, and the distances increase with the increasing remoteness of the C atoms from the bridge.

The “bite” angle θ of the *ansa*-bis(fluorenyl) ligand, which is best described as the dihedral angle between the mean planes of the two π -bonded rings, is equal to 73°. As expected, this angle is smaller than that found for the carbon-bridged Nd

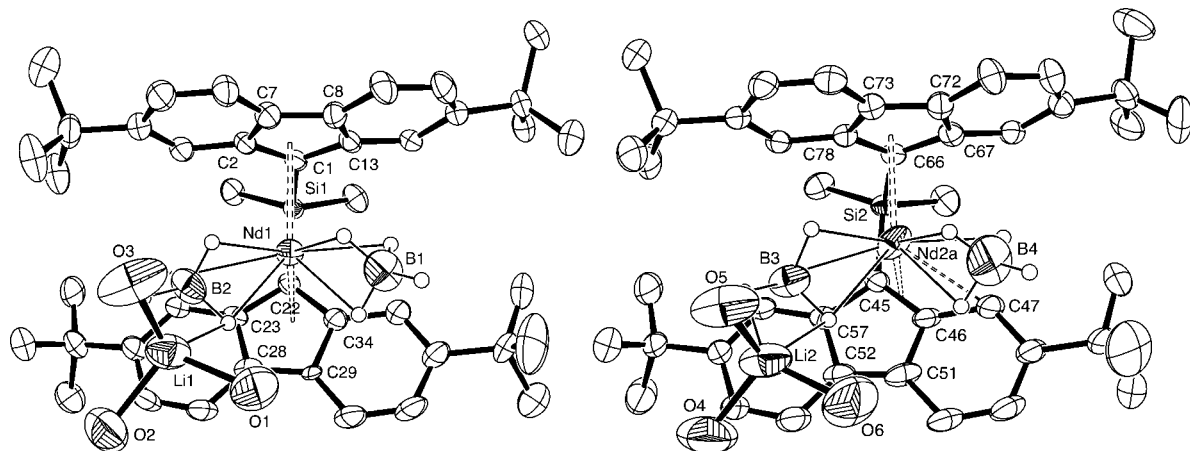


Figure 2. An ORTEP plot of **2**¹ (left) and **2**² (right) (ellipsoids scaled at 50%). The hydrogen atoms (except of the borohydrides) and the carbon atoms on the coordinated solvents have been omitted for clarity. O(2) belongs to the coordinated ether. Selected distances (Å) and angles (deg): Nd(1)–C(1) = 2.672(5); Nd(1)–C(2) = 2.710(5); Nd(1)–C(7) = 2.964(5); Nd(1)–C(13) = 2.934(5); Nd(1)–C(22) = 2.682(5); Nd(1)–C(23) = 2.964(5); Nd(1)–C(34) = 2.712(5); Nd(1)–C(29) = 2.969(5); Si(1)–C(22) = 1.867(5); Si(1)–C(1) = 1.861(5); Nd(1)–B(2) = 2.660(8); Nd(1)–B(1) = 2.59(1); B(2)–Nd(1)–B(1) = 100.3(3); C(22)–Si(1)–C(1) = 102.9(2); Nd(2A)–C(45) = 2.721(6); Nd(2A)–C(46) = 2.725(6); Nd(2A)–C(66) = 2.646(5); Nd(2A)–C(78) = 2.666(5); Nd(2A)–C(73) = 2.892(5); Si(2)–C(45) = 1.864(5); Si(2)–C(66) = 1.862(5); Nd(2A)–B(3) = 2.67(1); Nd(2A)–B(4) = 2.58(1); B(3)–Nd(2A)–B(4) = 100.4(4); C(45)–Si(2)–C(66) = 103.8(2).

Table 1. EBR Preparation Using 1/(nBu)(nOct)Mg Catalysts^a

run	[Nd] (μM)	Mg/Nd	time (h)	yield (g)	activity (kg/mol·h)	M_n^b (g/mol)	PDI	% But in polymer ^c	microstructure ^c (mol %)			T_g ($^{\circ}\text{C}$)
									trans-1,4	vinyl	trans-1,2-cyclohexane	
1	210	5	3	11.0	87	46200	1.60	26.7	31.8	35.2	33.0	-36.0
2	217	2	3	12.6	97	74800	1.54	25.3	31.9	31.9	36.1	-33.0
3 ^d	195	2	4	8.5	36	110000	2.70	19.3	27.6	28.4	44.0	-37.0
4	102	10	3	7.5	123	33300	1.68	28	32.3	38.9	28.8	-35.3
5	87	2	1	25.6	492	297000	3.16	12.9	25.3	39.6	35.1	-36.0
6	88	2	2.75	31.7	218	281000	1.92	30.8	29.6	50.3	20.2	-45.6

^a Polymerization conditions. Runs 1-4: 200 mL of toluene (run 3: 300 mL), 80 $^{\circ}\text{C}$, 4 bar, 30 mol % of butadiene in feed. Runs 5 and 6: 600 mL, 80 $^{\circ}\text{C}$ with the respective feed: 24.95 g of ethylene, 8.1 g of butadiene (14.4 mol %) and 24.35 g of ethylene, 22.6 g of butadiene (32.5 mol %). ^b By GPC in THF vs polystyrene standards. ^c Determined using ^1H and ^{13}C NMR analyses. ^d Using the chloride precursor $\{(\text{Me}_2\text{Si}(\text{C}_{13}\text{H}_8)_2)\text{NdCl}\}$ according to reference.⁸

complexes $(\text{L}^2)\text{Nd}(\text{allyl})(\text{THF})$ and $(\text{L}^3)\text{Nd}(\text{allyl})(\text{THF})$ ¹⁵ where $\theta \approx 84^{\circ}$.

Finally, the Nd-B distances are similar to those found in a related anionic Nd borohydride: $\{(\text{Flu}-\text{CPh}_2-\text{Cp})\text{Nd}(\text{BH}_4)_2\text{-K}[\text{18-C-6}]\}_2(\mu\text{-dioxane})$.¹⁷

Unlike the chloride silylene-bridged bisfluorenyl analogue and despite of the paramagnetism of neodymium, complex **1** was characterized by ^1H NMR spectroscopy. Broad resonances were observed but the signals were assigned easily because of the high increase of the spectral width in comparison with a ^1H NMR spectrum of a diamagnetic compound. The BH_4 signal was observed at low field (δ : 97.5 ppm) and the integral of this signal shows the presence of two borohydrides for one ansa-silylene-bridged ligand which confirm the formation of an ate complex.

tert-Butyl substituents were introduced on fluorenyl ligands with the aim of investigating ligand substituent effects on cyclocopolymerization mechanisms.

With the bis(*t*Bu₂-fluorenyl) silylene bridge, crystallization of THF/ether solutions ended up in a compound displaying two different molecules in the unit cell. The X-ray data were best modeled with one molecule being (*t*Bu₂Flu-SiMe₂-*t*Bu₂Flu)Nd-(BH₄)₂Li(THF)₂(Et₂O) (**2**¹) and the other (*t*Bu₂Flu-SiMe₂-*t*Bu₂Flu)Nd-(BH₄)₂Li(THF)₃ (**2**²). Figure 2 displays ORTEP plots of **2**¹ (left) and **2**² (right), respectively.

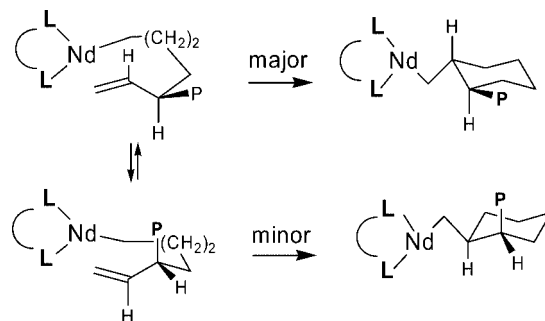
The X-ray data are not of a very good quality; however, we feel that the geometry around Nd is accurate enough for discussion. An important feature is that the solid-state geometries of **2**¹ and **2**² are significantly different from each other and also significantly different from that of **1**.

In **2**¹ and **2**², there are only two short Nd-C bonds to each fluorenyl ligands (Nd(1)-C(1)/Nd(1)-C(2) and Nd(1)-C(22)/Nd(1)-C(34) for **2**¹; Nd(2A)-C(66)/Nd(2A)-C(78) and Nd(2A)-C(45)/Nd(2A)-C(46) for **2**²). In **2**¹, there are two distances (Nd(1)-C(8) and Nd(1)-C(28)) that are not in the bonding range as defined earlier and thus the complex is best described as bis- $[\eta^4]$.

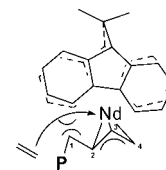
In one of the fluorenyl rings of **2**², there are only two Nd(2A)-C(5-membered ring) bonds, the other distances being above 3.23 Å. The Nd(2A) atom is even closer from C(47), which belongs to a 6-membered ring (distance = 3.19 Å). Thus, the Nd atom in **2**² is much tilted away from the center of one 5-membered ring, and the bonding situation of Nd is best described as $[\eta^3, \eta^2]$.

The ligand "bite" angles θ in **2**¹ and **2**² are also different since the dihedral angles between the fluorene planes (see above) are $\theta = 78^{\circ}$ for **2**¹ and $\theta = 86^{\circ}$ for **2**². Thus, the geometry is more open in **2**¹ and **2**² than in **1**. Steric crowding and in particular steric repulsion between the *t*-Bu groups lying above one another might be responsible for this difference in "bite" angles.

The very fact that **2**¹ and **2**² are found in the same unit cell implies that the energy difference between these two forms is small and that the activation energy should be low. Thus, the

Scheme 1. Model of Diastereoselective *trans*-1,2-Cyclohexane Formation

Scheme 2. Insertion of Ethylene in the Nd-C(2) Bond

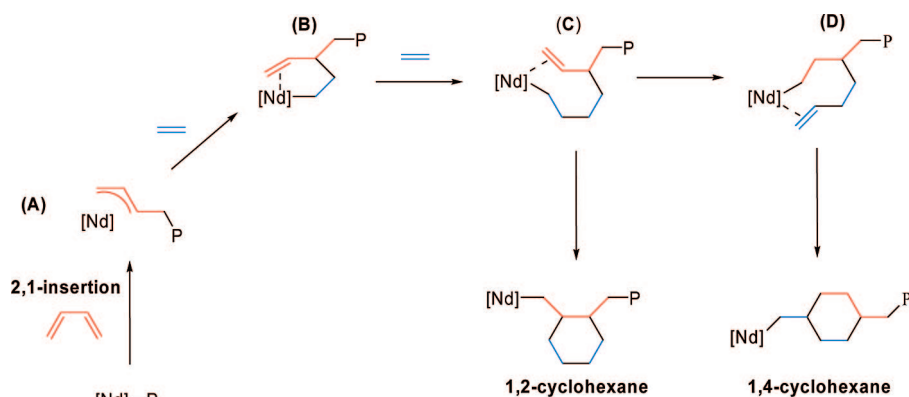


observed geometries might be due to packing effects and there may be some flexibility in the conformation of the complex in solution.

Finally, the Nd-B distances and B-Nd-B angles are quite similar to those in $\{(\text{Flu}-\text{CPh}_2-\text{Cp})\text{Nd}(\text{BH}_4)_2\text{-K}[\text{18-C-6}]\}_2(\mu\text{-dioxane})$.¹⁷

Cyclocopolymerization of Ethylene with Butadiene. The formation of active neutral lanthanidocene species can be performed *in situ* by a simple alkylation of a metallocene precursor. It is the route that we have chosen for practical reasons, mainly in relation with the lack of stability of alkyl species. Recently, it was shown that borohydride lanthanidocenes are efficient precursors toward active species for olefin polymerization.¹⁰ The copolymerization of ethylene with butadiene was performed by using respectively complexes **1** and **2** in combination with butyl-octylmagnesium (*n*Bu)(*n*Oct)Mg. The investigation of catalyst **1**/(*n*Bu)(*n*Oct)Mg for copolymerization of ethylene with butadiene is reported in Table 1. The new catalyst was very efficient and EBR were produced with high activity. Glass transition temperatures ($T_g = -33$ to -45 $^{\circ}\text{C}$) are in agreement with expected thermal properties for EBR.⁸ Comparison of borohydride and chloride precursors (runs 2 and 3) showed the higher efficiency of the borohydride complex **1** both in terms of activity ($\times 2.7$) and butadiene content in copolymers. As expected with neodymium metallocene catalysts used in a presence of a dialkylmagnesium compound, molecular weights were mainly controlled by reversible chain transfer reaction to magnesium. Molecular weights were increased by decreasing the concentration of magnesium (run 1 and 2) while keeping low polydispersity index (1.5-1.6). It is interesting to

Scheme 3. Mechanisms of Cyclization

Table 2. Cyclocopolymerization of Ethylene with Butadiene Using 2/(*n*Bu)(*n*Oct)Mg Catalyst System^a

run	[Nd] (μM)	time (h)	yield (g)	activity (kg/mol·h)	M_n^c (g/mol)	PDI	% But in polymer ^d	microstructure ^d (mol-%)				T_g ($^{\circ}\text{C}$)	
								<i>trans</i> -1,4	vinyl	<i>trans</i> -1,2-cyclohexane	<i>cis</i> -1,2-cyclohexane		<i>trans</i> -1,4-cyclohexane
7	256	1.7	9.19	107	11900	1.65	12.8	17.5	20.2	41.9	5.5	14.7	-33.6
8	269	2.2	9.74	83	27000	1.52	21.6	19.2	32.8	34.3	4.2	9.6	-35.7
9	247	4	7.61	38	31600	1.69	32.1	21.5	57.5	19.0	2.0	nd	-28.3
10 ^b	272	6.3	8.9	26	1600	1.56	10.2	25.4	7.6	45.9	5.2	15.9	nd

^a Polymerization conditions: 200 mL of toluene, Mg/Nd = 5, 80 $^{\circ}\text{C}$, 4 bar with the following feeds. Run 7: 10 mol % butadiene. Run 8: 20 mol % butadiene. Run 9: 30 mol % butadiene. nd: not determined. ^b 2 bar, 10 mol % butadiene. ^c By GPC in THF vs polystyrene standards. ^d Determined using ¹H and ¹³C NMR analyses.

note that, using complex **1**, it was possible to perform polymerization at lower concentration of neodymium. Decrease of neodymium concentration resulted in an increase of activity (runs 2 and 4) which can be attributed to lower interaction between neodymium species. Actually, it is well-known that bimolecular interaction can lead to dormant or inactive species. Increase of monomer concentration (runs 5 and 6) resulted to a high increase in both activity and molecular weight. In addition it is important to note that the later experiments were performed in a batch reactor which is then not continuously feed with a mixture of monomers as in the case of polymerization performed at lower pressure. Conversions in both monomers were very high, respectively 70% of butadiene and 80% of ethylene (run 5) and 64% of butadiene and 70% of ethylene (run 6). This means that initial activities were certainly much higher than average activity reported in Table 1. In conclusion catalyst **1**/(*n*Bu)(*n*Oct)Mg appears as a very valuable system for production of EBR.

Mechanism of formation of 1,2-cyclohexane rings is given in Scheme 3. The intramolecular cyclization occurred with exo regioselectivity as evidence by the absence of cycloheptane units. At this point it appears useful to discuss stereochemistry of cyclohexane rings. Actually, a high diastereoselective cyclohexane formation occurred leading to original *trans*-1,2-cyclohexane units. The high stereoselectivity of the intramolecular cyclization seems to be correlated to a pseudoequatorial position of the polymer growing chain which reduced interactions of this chain with the bulky fluorenyl ligands (Scheme 1).¹⁸ *trans*-1,2-Stereoselectivity is indeed in agreement with works from Stille et al., who have reported that intramolecular cyclization of 5-methyl hept-6-en-1-yl ligand of a titanocene complex provided, after quenching with HCl, 1,2-dimethylcyclohexane with 99:1 *trans*-*cis* selectivity.¹⁹ In the case of copolymerization of ethylene with cyclohexene an opposite selectivity was observed. Recently, Nomura and co-workers succeeded in copolymerizing ethylene with cyclohexene using half-titanocenes containing aryl-oxo ligands Cp^{*}TiCl₂(OAr).²⁰ Because of the *cis* insertion of olefin units, the microstructure of cyclohexane unit was exclusively *cis*-1,2.

Table 3. Cyclic Unit and Assignments of Relayed ¹³C Chemical Shifts

Chemical structure	Carbon type	Chemical Shift (ppm)
A	CH	41.98
	α - <i>trans</i> -1,2	33.94
	β - <i>trans</i> -1,2	26.97
	γ - <i>trans</i> -1,2	30.58
	α' - <i>trans</i> -1,2	32.26
	β' - <i>trans</i> -1,2	26.67
B	CH	39.71
	α - <i>cis</i> -1,2	28.18
	β - <i>cis</i> -1,2	29.30
	α' - <i>cis</i> -1,2	30.58
	β' - <i>cis</i> -1,2	24.26
C	CH	38.45
	α - <i>trans</i> -1,4	37.95
	β - <i>trans</i> -1,4	27.38
	γ - <i>trans</i> -1,4	30.44
	α' - <i>trans</i> -1,4	33.94

Investigation of complex **2** revealed that the tertio-butyl substitution in positions 2 and 7 of fluorenyl ligands has influenced the microstructure of copolymers. Copolymerization

experiments using the catalyst **2**/(*n*Bu)(*n*Oct)Mg are given in Table 2. An efficient butadiene insertion was observed leading to a good correlation between monomer feed and polymer composition. However, this catalyst displayed lower activity than the former catalyst system **1**/(*n*Bu)(*n*Oct)Mg for copolymerization of ethylene with butadiene (compare runs 1 and 9). More interestingly, the regioselectivity of butadiene insertion was modified. The selectivity for 1,2-units versus 1,4-units was significantly increased. Since 1,2-units are involved in cyclization mechanisms, this selectivity can be easily measured by the decrease of the amount of *trans*-1,4-units (runs 1 and 9). More generally, using *ansa*-bis(flourenyl)neodymium catalysts, a remarkable regioselectivity (2,1-insertion) for butadiene insertion was observed since most neodymium metallocenes lead to 1,4-insertion. To account for this high regioselectivity we assume that the steric hindrance of bis(flourenyl) ligands causes repulsion of the growing polymer which is moved away from the coordination site (based on a chain migratory insertion mechanism) enabling coordination of ethylene and insertion of this monomer in the neodymium–C(2) bond (Scheme 2).

The increase of ring structures content together with decrease of vinyl content (1,2-units) by decreasing the butadiene content in the feed (runs 7–9) or by decreasing the concentration of both monomers (run 10) are in agreement with an intramolecular cyclization mechanism involving one butadiene and two ethylene units (Scheme 3). As in the case of catalysts based on complex **1**, complex **2** provided 1,2-cyclohexane rings and a high *trans*-1,2-stereoselectivity (slightly lower than for the former catalyst) was observed (approximately 90/10 *trans/cis*). Unexpectedly, a new microstructure was detected in the polymer backbone using ¹³C NMR. This microstructure was fully characterized using 2D NMR ¹H–¹H and ¹H–¹³C with direct and long-range correlations (see selected spectra in Supporting Information). It corresponds to unprecedented 1,4-cyclohexane rings. The chemical shift (CH and CH₂) of the different rings encounter in the backbone of the new ethylene/butadiene copolymers are given in Table 3 (see selected spectra in Supporting Information). The formation of 1,4-cyclohexane was attributed to the isomerization of the polymer chain in species **C** (Scheme 3) via a β-H transfer on the pendant vinyl unit. A new intermediate (**D**) was then formed and the intramolecular insertion of the vinyl unit in species **D** provided the 1,4-cyclohexane ring.

In summary, *ansa*-bis(flourenyl)neodymium metallocene catalysts proved to be efficient catalyst for cyclocopolymerization of ethylene with butadiene leading to a new class of elastomers called EBR. These elastomers are characterized by a polyethylene skeleton incorporating unsaturated groups (*trans* double bond and pendant vinyl units) and rings (1,2- and 1,4-cyclohexane units). The presence of these rings greatly influences the thermal properties of the materials. Glass transition temperatures are adjusted by controlling polymerization conditions and are typically in the range of –45 to –30 °C.

Acknowledgment. The authors thank the Manufacture Michelin for support and useful discussions, in particular with Dr. F. Barbotin and Dr. P. Robert. The authors are grateful to Xavier-Frédéric Le Goff for his help in determining structure of organometallic complexes.

Supporting Information Available: Figures showing selected NMR spectra of polymers and tables of crystal data for **1** and **2** and X-ray crystallographic data files in CIF format for complexes.

These materials are available free of charge via the Internet at <http://pubs.acs.org>.

References and Notes

- (1) (a) Mulhaupt, R. *Macromol. Chem. Phys.* **2003**, *204*, 289–327. (b) Galli, P.; Vecellio, G. *J. Polym. Sci., Part A: Polym. Chem.* **2004**, *42*, 396–415. (c) Kaminsky, W. *J. Polym. Sci., Part A: Polym. Chem.* **2004**, *42*, 3911–3921.
- (2) (a) Kaminsky, W.; Bark, A.; Arndt, M. *Makromol. Chem., Macromol. Symp.* **1991**, *47*, 83–93. (b) Kaminsky, W.; Beulich, I.; Arndt-Rosenau, M. *Macromol. Symp.* **2001**, *173*, 211–225. (c) Kaminsky, W.; Hoff, M.; Derlin, S. *Macromol. Chem. Phys.* **2007**, *208*, 1341–1348.
- (3) (a) Resconi, L.; Waymouth, R. M. *J. Am. Chem. Soc.* **1990**, *112*, 4953–4954. (b) Cavallo, L.; Guerra, G.; Corradini, P.; Resconi, L.; Waymouth, R. M. *Macromolecules* **1993**, *26*, 260–267. (c) Coates, G. W.; Waymouth, R. M. *J. Am. Chem. Soc.* **1993**, *115*, 91–98. (d) Kim, I.; Shin, Y. S.; Lee, J. K. *J. Polym. Sci., Part A: Polym. Chem.* **2000**, *38*, 1590–1598. (e) Kim, I.; Shin, Y. S.; Lee, J. K.; Cho, N. J.; Lee, J. O.; Won, M. S. *Polymer* **2001**, *42*, 9393–9403. (f) Choo, T. N.; Waymouth, R. M. *J. Am. Chem. Soc.* **2002**, *124*, 4188–4189. (g) Naga, N.; Imanishi, Y. *Macromol. Chem. Phys.* **2002**, *203*, 771–777. (h) Hustad, P. D.; Tian, J.; Coates, G. W. *J. Am. Chem. Soc.* **2002**, *124*, 3614–3621. (i) Napoli, M.; Costabile, C.; Cavallo, G.; Longo, P. *J. Polym. Sci., Part A: Polym. Chem.* **2006**, *44*, 5525–5532. (j) Takeuchi, D.; Matsuura, R.; Park, S.; Osakada, K. *J. Am. Chem. Soc.* **2007**, *129*, 7002–7003.
- (4) (a) Galimberti, M.; Albizzati, E.; Abis, L.; Bacchilega, G. *Makromol. Chem.* **1991**, *192*, 2591–2601. (b) Pragliola, S.; Milano, G.; Guerra, G.; Longo, P. *J. Am. Chem. Soc.* **2002**, *124*, 3502–3503. (c) Choo, T. N.; Waymouth, R. M. *J. Am. Chem. Soc.* **2003**, *125*, 8970–8971. (d) Longo, P.; Napoli, M.; Pragliola, S.; Costabile, C.; Milano, G.; Guerra, G. *Macromolecules* **2003**, *36*, 9067–9074. (e) Longo, P.; Pragliola, S.; Milano, G.; Guerra, G. *J. Am. Chem. Soc.* **2003**, *125*, 4799–4803. (f) Pragliola, S.; Costabile, C.; Magrino, M.; Napoli, M.; Longo, P. *Macromolecules* **2004**, *37*, 238–240. (g) Pragliola, S.; Costabile, C.; Napoli, M.; Guerra, G.; Longo, P. *Macromol. Symp.* **2006**, *234*, 128–138. (h) Pellegrino, M.; Costabile, C.; Grisi, F.; Pragliola, S. *Eur. Polym. J.* **2008**, *44*, 2625–2628.
- (5) Cavallo, G.; Venditto, V.; Annunziata, L.; Pragliola, S.; Longo, P.; Guerra, G. *Polymer* **2005**, *46*, 2847–2853.
- (6) Boisson, C.; Monteil, V.; Thuilliez, J.; Spitz, R.; Monnet, C.; Llauro, M.-F.; Barbotin, F.; Robert, P. *Macromol. Symp.* **2005**, *226*, 17–23.
- (7) (a) Barbotin, F.; Monteil, V.; Llauro, M.-F.; Boisson, C.; Spitz, R. *Macromolecules* **2000**, *33*, 8521–8523. (b) Thuilliez, J.; Monteil, V.; Spitz, R.; Boisson, C. *Angew. Chem., Int. Ed.* **2005**, *44*, 2593–2596.
- (8) Monteil, V.; Spitz, R.; Barbotin, F.; Boisson, C. *Macromol. Chem. Phys.* **2004**, *205*, 737–742.
- (9) Monteil, V.; Spitz, R.; Boisson, C. WO 2004/ 035639, Michelin Recherche et Technique S.A. and Atofina Research.
- (10) (a) Bonnet, F.; Visseaux, M.; Pereira, A.; Barbier-Baudry, D. *Macromolecules* **2005**, *38*, 3162–3169. (b) Thuilliez, J.; Spitz, R.; Boisson, C. *Macromol. Chem. Phys.* **2006**, *207*, 1727–1731. (c) Visseaux, M.; Chenal, T.; Roussel, P.; Mortreux, A. *J. Organomet. Chem.* **2006**, *691*, 86–92. (d) Terrier, M.; Visseaux, M.; Chenal, T.; Mortreux, A. *J. Polym. Sci., Part A: Polym. Chem.* **2007**, *45*, 2400–2409.
- (11) (a) Barbier-Baudry, D.; Blacque, O.; Hafid, A.; Nyassi, A.; Sitzmann, H.; Visseaux, M. *Eur. J. Inorg. Chem.* **2000**, 2333–2336. (b) Cendrowski-Guillaume, S. M.; Le Gland, G.; Nierlich, M.; Ephritikhine, M. *Organometallics* **2000**, *19*, 5654–5660.
- (12) Cordero, B.; Gomez, V.; Platero-Prats, A. E.; Reves, M.; Echeverria, J.; Cremades, E.; Barragan, F.; Alvarez, S. *Dalton Trans.* **2008**, 2832–2838.
- (13) Kirillov, E.; Saillard, J.-Y.; Carpentier, J.-F. *Coord. Chem. Rev.* **2005**, *249*, 1221–1248.
- (14) Qian, C.; Nie, W.; Sun, J. *Organometallics* **2000**, *19*, 4134–4140.
- (15) Rodrigues, A.-S.; Kirillov, E.; Lehmann, C. W.; Roisnel, T.; Vuillemin, B.; Razavi, A.; Carpentier, J.-F. *Chem.–Eur. J.* **2007**, *13*, 5548–5565.
- (16) Lee, M. H.; Hwang, J.-W.; Kim, Y.; Kim, J.; Han, Y.; Do, Y. *Organometallics* **1999**, *18*, 5124–5129.
- (17) Qian, C.; Nie, W.; Sun, J. *J. Organomet. Chem.* **2001**, *626*, 171–175.
- (18) Young, J. R.; Stille, J. R. *Organometallics* **1990**, *9*, 3022–3025.
- (19) Young, J. R.; Stille, J. R. *J. Am. Chem. Soc.* **1992**, *114*, 4936–4937.
- (20) Wang, W.; Fujiki, M.; Nomura, K. *J. Am. Chem. Soc.* **2005**, *127*, 4582–4583.

MA9003852